Fabrication of Multiscale Surface-Chemical Gradients by Means of Photocatalytic Lithography

Nicolas Blondiaux,[†,‡] Stefan Zürcher,[‡] Martha Liley,*[,†] and Nicholas D. Spencer[‡]

Centre Suisse d'Electronique et de Microtechnique, SA, Jacquet Droz 1, CH-2000 Neuchâtel, Switzerland, and Laboratory for Surface Science and Technology, Department of Materials, ETH Zurich, Wolfgang-Pauli-Strasse 10, CH-8093 Zurich, Switzerland

Received November 1, 2006. In Final Form: January 19, 2007

We describe a new method for the fabrication of surface-chemical gradients. A film of titanium dioxide is brought into close proximity to a uniformly monolayer-covered surface and exposed to UV light to produce oxygen radicals. The use of a gradated grayscale mask between the UV source and the TiO_2 allows the production of surface-chemical gradients via oxidation of the monolayer. The technique is demonstrated on gold surfaces bearing alkanethiol SAMs. Oxidation and subsequent replacement of the oxidized thiols has been used to produce surface-chemical gradients with lengths on the submillimeter to centimeter scales. The oxidation, removal, and replacement of the thiols during the process have been demonstrated by means of XPS. This oxidative process may be applied to other surface chemistries. Similarly, other shapes and slopes of gradients may be produced, depending on the photomask employed.

Introduction

Surface-chemical gradient fabrication constitutes a very active field of research due to the utility of gradients in innumerable research applications. Surface gradients are useful tools for the combinatorial investigation of cell behavior or in biochemical assays because a vast number of surface-chemistry combinations can be screened for a single sample.[1,2] In a different field, wettability gradients can be used to control the motion and positioning of liquid drops on surfaces.[3−5] The design of gradients is, however, very dependent on the envisaged application. In high-throughput studies, the critical parameter is the number of conditions that can be screened on a single sample, whereas in the case of motion and positioning of liquids, emphasis is put on the slope of the gradients. In both situations, the length and slope of the gradient are important parameters.

Several approaches to creating chemical gradients have already been reported, such as the use of cross diffusion of thiol solutions through a polysaccharide matrix[6,7] or the gradual immersion of a gold-coated substrate in a dilute thiol solution.[8] Thiol composition gradients have also been generated by microcontact printing a gold surface with a PDMS stamp having a thickness gradient.[5] The length of the gradients produced with the techniques mentioned above is generally between a millimeter and a few centimeters. For the fabrication of submillimeter gradients, very different approaches have been reported. Choi et al. used microcontact printing to create gradients in silane surface concentration.[9] Gradients have also been created by selectively desorbing thiols using electrochemistry.[10] Fuierer et al. reported an STM-based technique permitting the controlled desorption of thiols by varying both the scan rate and the voltage applied.[11] The techniques based on microcontact printing have great flexibility with regard to the shape and length of the gradient.[9] Nevertheless, the use of PDMS as an elastomeric stamp may pose problems for some applications as a result of the possibility of surface contamination.[12] Approaches based on SPM techniques also offer good control over the properties of the gradients, but serial techniques such as these are inevitably limited in terms of throughput. Thus there is a need for new parallel techniques for the fabrication of short gradients.

We describe a technique that allows the generation of both long as well as short surface-chemical gradients. We have focused on the use of light to produce the gradients, using titanium dioxide (TiO_2) remote photocatalytic oxidation. In this technique, also called photocatalytic lithography, a titanium dioxide layer is held in close proximity to a monolayer-covered surface and irradiated with UV light. Radicals created in the TiO_2 layer diffuse across the air gap and react with organics adsorbed on the nearby surface. The degradation of silane and thiol self-assembled monolayers (SAMs) by means of photocatalytic lithography has already been demonstrated.[13,14] It has been used to pattern surfaces,[14,15] with a photomask being employed to illuminate the surface selectively and locally degrade the adsorbed species. In this study, we have combined photocatalytic lithography with grayscale lithography to degrade a thiol SAM gradually and produce a surface-chemical gradient.

The technique used is shown in Figure 1: a TiO_2-coated slide was placed above the substrate to be modified with a 60 μm intervening air gap. Upon UV illumination of the slide, oxidizing

* To whom correspondence should be addressed. E-mail: martha.liley@csem.ch. Tel: +41 32 720 51 84. Fax: +41 32 720 57 40.

† Centre Suisse d'Electronique et de Microtechnique.

‡ ETH Zurich.

(1) Meredith, J. C.; Karim, A.; Amis, E. J. *MRS Bull.* **2002**, *27*, 330−335.
(2) Herbert, C. B.; McLernon, T. L.; Hypolite, C. L.; Adams, D. N.; Pikus, L.; Huang, C. C.; Fields, G. B.; Letourneau, P. C.; Distefano, M. D.; Hu, W. S. *Chem. Biol.* **1997**, *4*, 731−737.
(3) Daniel, S.; Chaudhury, M. K.; Chen, J. C. *Science* **2001**, *291*, 633−636.
(4) Gallardo, B. S.; Gupta, V. K.; Eagerton, F. D.; Jong, L. I.; Craig, V. S.; Shah, R. R.; Abbott, N. L. *Science* **1999**, *283*, 57−60.
(5) Kraus, T.; Stutz, R.; Balmer, T. E.; Schmid, H.; Malaquin, L.; Spencer, N. D.; Wolf, H. *Langmuir* **2005**, *21*, 7796−7804.
(6) Liedberg, B.; Tengvall, P. *Langmuir* **1995**, *11*, 3821−3827.
(7) Liedberg, B.; Wirde, M.; Tao, Y. T.; Tengvall, P.; Gelius, U. *Langmuir* **1997**, *13*, 5329−5334.
(8) Morgenthaler, S.; Lee, S. W.; Zürcher, S.; Spencer, N. D. *Langmuir* **2003**, *19*, 10459−10462.
(9) Choi, S. H.; Newby, B. M. Z. *Langmuir* **2003**, *19*, 7427−7435.
(10) Bohn, P.; Plummer, S.; Wang, Q.; Coleman, B.; Swint, A.; Castle, P. *Abstr. Pap. Am. Chem. Soc.* **2003**, *225*, U687.
(11) Fuierer, R. R.; Carroll, R. L.; Feldheim, D. L.; Gorman, C. B. *Adv. Mater.* **2002**, *14*, 154−157.
(12) Csucs, G.; Kunzler, T.; Feldman, K.; Robin, F.; Spencer, N. D. *Langmuir* **2003**, *19*, 6104−6109.
(13) Tatsuma, T.; Tachibana, S.; Fujishima, A. *J. Phys. Chem. B* **2001**, *105*, 6987−6992.
(14) Notsu, H.; Kubo, W.; Shitanda, I.; Tatsuma, T. *J. Mater. Chem.* **2005**, *15*, 1523−1527.
(15) Kubo, W.; Tatsuma, T.; Fujishima, A.; Kobayashi, H. *J. Phys. Chem. B* **2004**, *108*, 3005−3009.

10.1021/la063186+ CCC: $37.00
Published on Web 02/27/2007

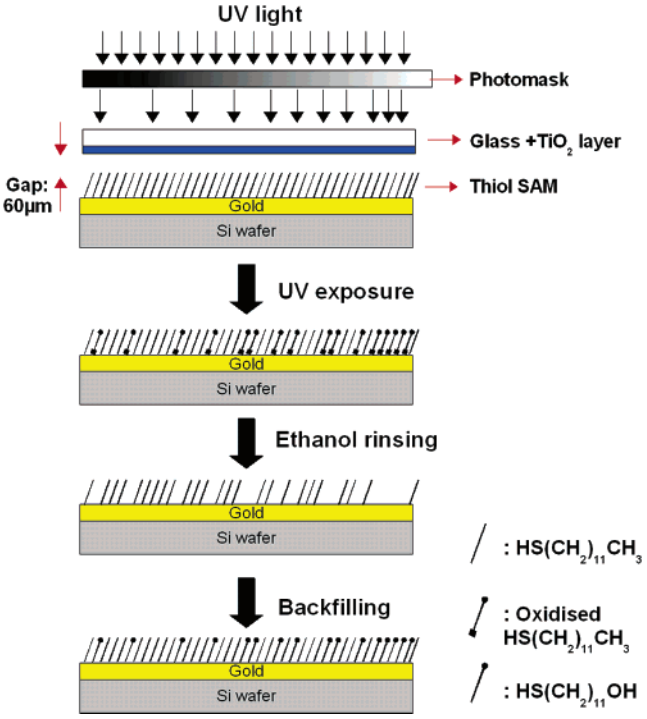

Figure 1. Remote photocatalytic oxidation of a thiol SAM under a gradient of UV illumination and subsequent backfilling with a second component.

radicals were created in the TiO_2 film as a result of its photocatalytic properties. The use of a photomask with a gray-tone gradient yielded a gradual variation of UV intensity along the TiO_2 film. Because the photocatalytic activity of TiO_2 depends on the intensity of the UV illumination,[16] the intensity variation was transposed into an oxygen radical concentration gradient, which led to a gradient in the oxidation of the substrate surface.

Materials and Methods

Formation of Thiol SAMs. The substrates used for the experiments were prepared by evaporating 30 nm of chromium followed by 120 nm of gold (99.99%, Umicore, Bösingen, Switzerland) onto silicon wafers (type P/Bor, ⟨100⟩, Siltronix, Archamps, France) using an e-beam evaporator (Leybold). The thiols used were $(CH_3(CH_2)_{11}$-SH (dodecanethiol 98+%) and $(HO(CH_2)_{11}SH$ (11-mercapto-1-undecanol 97+%), both purchased from Aldrich Chemicals (Milwaukee, WI). 1H,1H,2H,2H-Perfluorodecanethiol was purchased from Fluorous Technologies Inc. (Pittsburgh, PA). Ethanol (UVasol for spectroscopy) was obtained from Merck. The starting SAM was made by placing the gold-coated substrates overnight in a 1 mM dodecanethiol solution. The surface was then rinsed twice in ethanol and blown dry with nitrogen.

Photocatalytic Remote Oxidation. The photocatalytic layer was made by spin coating a TiO_2 nanoparticle suspension onto a clean glass slide. The TiO_2 nanoparticles were in the anatase form and were 7 nm in diameter. The TiO_2 suspension (STS-01) was kindly supplied by Ishihara Sangyo Gaisha, Ltd. (Yokkaichi, Japan). A small amount of poly(*N*-vinyl pyrrolidone) (K90 from Fluka (Buchs, Switzerland)) was added to the suspension to improve the quality of the film and avoid the formation of cracks during film formation. The final solution contained 10 wt % of TiO_2 and 0.2 mg/mL poly(*N*-vinyl pyrrolidone). Glass slides were cleaned using piranha solution (4:1 v/v H_2SO_4/H_2O_2) for 10 min at 120 °C and rinsed in flowing water (MilliQ 185 plus, Millipore AG, Switzerland). ***Attention:*** *Piranha solution reacts violently with all organics and should be handled with care*. The solution was then spin coated at 6000 rpm onto the cleaned glass slide. To remove all traces of organic compounds present in the layer, the TiO_2-coated slides were then calcined at 400 °C for 1 h in an oven (Nabertherm, model L15/12/P320, Bremen, Germany). Because the anatase-rutile phase transition in TiO_2 occurs at temperatures above 600 °C,[17] we do not expect any phase transition due to this treatment. The cleaning of the TiO_2 layer proved to be an important issue. Before each experiment, the TiO_2 surfaces were cleaned in an oxygen plasma for 15 min using an rf power of 30 W and a pressure of 0.250 Torr (Plasmalab 80 plus, Oxford Instruments). The TiO_2-coated glass slides were then exposed to UV for 1 h. The irradiance of the lamp used (Oriel 300 W solar ultraviolet simulator, Lot-Oriel) was 17 mW/cm^2 at a wavelength of 365 nm. The photomask used for photocatalytic lithography was custom designed and fabricated by Photronics Ltd. (Manchester, U.K.). The lengths of the gray-tone gradients were 1.8 cm and 720 μm for the long and short gradients, respectively. The short gradients were repeated several times along the photomask. The grayscale gradients were not continuous but comprised 12 distinct gray tones.

After the remote photocatalytic oxidation, the samples were rinsed in ethanol. Backfilling was made by dipping the samples for 10 min in a 1 mM solution of 11-mercapto-1-undecanol or 1H,1H,2H,2H-perfluorodecanethiol dissolved in ethanol. The samples were then rinsed again in ethanol.

Contact-Angle Measurements. The wettability changes of the surfaces were characterized by measuring the contact angle of sessile water droplets as a function of their position along the gradient. Static water contact angles were determined using a DSA10 drop shape analysis system provided by Krüss (Hamburg, Germany).

Standard deviations were calculated using eight series of measurements (two series per sample on four distinct samples) and were used to calculate both the standard error of the mean and the confidence intervals. The confidence intervals were calculated using the Student's *t* distribution instead of the normal distribution because of the small number of samples considered. The error bars shown on the graph correspond to an 80% confidence interval.

XPS Measurements. XPS analysis was performed using a VG Theta Probe spectrophotometer (Thermo Electron Corporation, West Sussex, U.K.) equipped with a concentric hemispherical analyzer and a 2D channel plate detector with 112 energy channels and 96 angle channels. Spectra were acquired at a base pressure of 10^{-9} mbar or below using a monochromatic Al Kα source with a spot size of 300 μm. The instrument was run in the standard lens mode with electrons emitted at 53° with respect to the surface normal and an acceptance angle of ±30°. The analyzer was used in the constant-analyzer-energy mode. Pass energies used for survey scans and detailed scans were 200 and 100 eV, respectively for Au 4f, C 1s, O 1s, S 2p, and F 1s. Under these conditions, the energy resolutions (fwhm) measured on Au $4f_{7/2}$ are 1.95 and 0.82 eV, respectively. Acquisition times were approximately 5 min for survey scans and 30 min (total) for high-energy-resolution elemental scans. These experimental conditions were chosen to obtain an adequate signal-to-noise ratio in a minimum time and to limit beam-induced damage. Under these conditions, sample damage was negligible, and reproducible analysis conditions were obtained on all samples. All recorded spectra were referenced to the Au $4f_{7/2}$ signal at 83.96 eV. Data were analyzed using the program CasaXPS (version 2.3.5 www.casaxps.com). The signals were fitted using Gaussian−Lorentzian functions and Tauc asymmetry in the case of gold and least-squares-fit routines following Shirley iterative background subtraction. Sensitivity factors were calculated using published ionization cross sections[18] corrected for the angular asymmetry[19] and the attenuation-length dependence on kinetic energy.

(16) Tatsuma, T.; Kubo, W.; Fujishima, A. *Langmuir* **2002**, *18*, 9632−9634.
(17) Ranade, M. R.; Navrotsky, A.; Zhang, H. Z.; Banfield, J. F.; Elder, S. H.; Zaban, A.; Borse, P. H.; Kulkarni, S. K.; Doran, G. S.; Whitfield, H. J. *Proc. Natl. Acad. Sci. U.S.A.* **2002**, *99*, 6476−6481.
(18) Scofield, J. H. *J. Electron Spectrosc. Relat. Phenom.* **1976**, *8*, 129−137.
(19) Reilman, R. F.; Msezane, A.; Manson, S. T. *J. Electron Spectrosc. Relat. Phenom.* **1976**, *8*, 389−394.

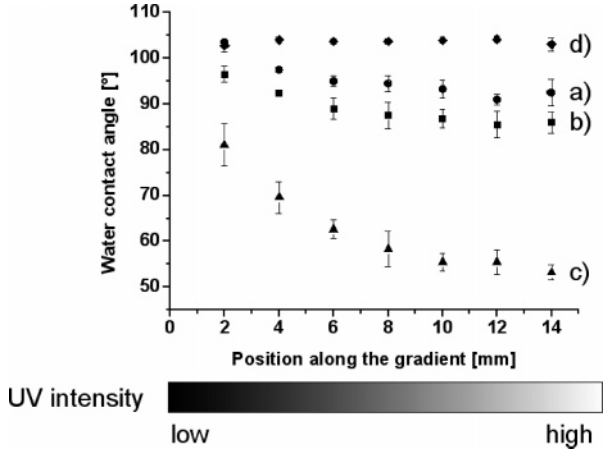

Figure 2. Water contact angles measured along the long gradient after different steps of the experiment. Results after (a) photocatalytic lithography, (b) photocatalytic lithography and rinsing with ethanol, (c) photocatalytic lithography, rinsing with ethanol, and backfilling with 11-mercapto-1-undecanol, and (d) rinsing a 1-dodecanethiol SAM with ethanol and backfilling with 11-mercapto-1-undecanol. The error bars correspond to an 80% confidence interval.

Results and Discussion

Gold-coated silicon wafers bearing a dodecanethiolate SAM were employed as substrates. A TiO_2-coated glass slide was placed on a 60 μm spacer on the gold surface, and the photomask was positioned above the assembly. Two kinds of gray-tone gradients were used: either a long 18 mm gray-tone gradient or a series of repeating short gradients, 720 μm long, as shown in Figure 4. The system was exposed to UV for 50 min, and the samples were then rinsed in ethanol. The SAM was backfilled by dipping the sample in a solution of 11-mercapto-1-undecanol. The long grayscale gradient was used initially to demonstrate the feasibility of the technique. The wettability gradients obtained were characterized by means of water contact angle measurements, performed after each step of the experiment. The results are presented in Figure 2.

Following the photocatalytic lithography step, the water contact angle was found to change only slightly along the gradient and was lower on the most exposed side of the sample. After the sample was rinsed with ethanol, a wettability gradient was observed, but the water-contact-angle changed only from 95 to 85°. The most hydrophilic part of the gradient corresponded to the most UV-exposed area. For comparison, a freshly prepared gold surface after rinsing in ethanol shows a water contact angle of 65°.[8] A much more pronounced gradient was obtained after backfilling the SAM with 11-mercapto-1-undecanol, when the water contact angle varied from 80 to 55°. The decrease in wettability was nonlinear, with the slope of the gradient decreasing toward the hydrophilic. A significant decrease was observed at distances between 2 and 8 mm from the low-UV-intensity end. At distances between 8 and 15 mm, the measurements were not significantly different, and a plateau was observed. To highlight the effect of photocatalysis, a control experiment was conducted where a homogeneous dodecanethiol SAM was not subjected to photocatalytic lithography but was rinsed with ethanol and backfilled with 11-mercapto-1-undecanol instead. As shown in Figure 2, no changes in contact angles were observed in this case.

XPS measurements were performed to gain a better understanding of the mechanism of photocatalytic degradation of the thiol SAM. Homogeneous samples were subjected to the process (without the gradient photomask) and XPS spectra measured at each step. The homogeneous sample thus corresponded to a position at the most hydrophilic end of the gradients. We mainly focused on the O 1s, C 1s, and S 2p regions of the spectrum. One critical step of the process was the backfilling of the oxidized SAM. The importance of this step was highlighted by backfilling the SAM with two different thiols: 11-mercapto-1-undecanol and 1H,1H,2H,2H-perfluorodecanethiol. When the SAM was backfilled with the perfluorinated thiol, the F 1s region of the spectrum was also measured.

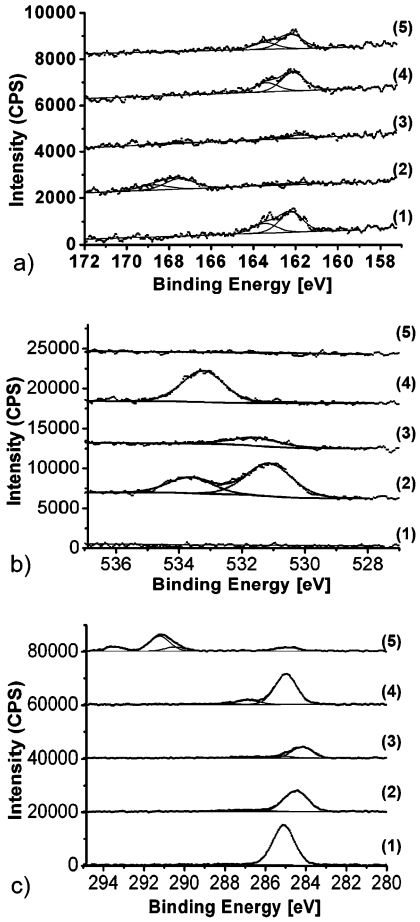

Figure 3. XPS spectra of (a) sulfur, (b) oxygen, and (c) carbon. The spectra were measured after each step of the process: (1) For the dodecanethiol SAM and following (2) photocatalytic lithography, (3) photocatalytic lithography and ethanol rinsing, (4) photocatalytic lithography, ethanol rinsing, and backfilling in 11-mercapto-1-undecanol, and (5) photocatalytic lithography, ethanol rinsing, and backfilling in 1H,H,2H,2H-perfluorodecanethiol. For clarity, the spectra are displaced along the *y* axis by 2000 CPS for S 2p, 6000 CPS for O 1s, and 20000 CPS for C 1s.

S2p spectra measured at each step of the process are shown in Figure 3a. For the dodecanethiol monolayer, one sulfur species was detected with a binding energy of the S $2p_{3/2}$ signal at 162.2 eV. After remote photocatalytic oxidation, a second sulfur peak appeared with a S $2p_{3/2}$ binding energy of 167.5 eV. Previous studies attributed this peak to the formation of sulfonate compounds.[20] After ethanol rinsing, the high-binding-energy sulfur peak disappeared as a result of the dissolution of the oxidized species in ethanol. Once the vacant sites were backfilled either with 11-mercapto-1-undecanol or 1H,1H,2H,2H-perfluorodecanethiol, the signal at 162.2 eV reappeared, confirming the adsorption of new thiols on the gold surface.

O 1s spectra are shown in Figure 3b for the same series of samples. As expected, no oxygen was detected for the dode-

(20) Brewer, N. J.; Janusz, S.; Critchley, K.; Evans, S. D.; Leggett, G. J. *J. Phys. Chem. B* **2005**, *109*, 11247−11256.

canethiol SAM. After remote photocatalytic oxidation, two peaks were observed: one at 531.1 eV and the other at 533.6 eV. Previous studies, focusing on the air oxidation of dodecanethiol, also reported the appearance of a peak at 531 eV.[21] The authors ascribed this peak to the formation of sulfonate species. As a comparison, the O 1s binding energy of 4-aminobenzenesulfonic acid was measured at 531.3 eV, and the S $2p_{3/2}$ binding energy was measured at 167.8 eV.[22] The second peak we observed may have arisen from a slight degree of oxidation of the alkyl chain on the thiol. Remote photocatalytic oxidation was already been reported to oxidize the alkyl chains of silane molecules efficiently.[23] Thus, there are two processes occurring in parallel during the experiment: the fast oxidation of the thiol headgroup to a sulfonate and the possibly slower oxidation of the alkyl chain. Slight oxidation of the gold surface also cannot be completely excluded. After ethanol rinsing, the amount of oxygen diminished significantly as a result of the dissolution of the sulfonate species. After backfilling with 11-mercapto-1-undecanol, a strong peak at 533.2 eV was observed again, confirming the adsorption of the hydroxyl-terminated thiol. When the SAM was backfilled with the perfluorinated thiol, no oxygen was detected.

C 1s spectra are shown in Figure 3c for the same series of samples. For the dodecanethiol SAM, a peak was observed at 285.1 eV, corresponding to the aliphatic carbon of dodecanethiol. After remote photocatalytic oxidation, a decrease in the peak intensity and a shift of 0.7 eV to lower binding energies were noticed. This effect was also reported by Willey et al. after air oxidation of dodecanethiol SAMs.[21] Ethanol rinsing led to a further decrease in the intensity of this peak. After backfilling with 11-mercapto-1-undecanol, the peak was observed again at 285 eV as a result of the adsorption of the new thiols. The shift in the C 1s peak is thought to be due to a slight shift in the surface potential of the gold as the electron-withdrawing S−Au bond is removed by oxidation and replaced by sulfonate species with little surface interaction (the molecules being subsequently held in place by interchain van der Waals interactions). The surface potential and C 1s peak return to the initial value following backfilling with the second thiol. Related effects have been observed in the case of fluorinated thiol gradients.[24]

Following backfilling with the perfluorinated thiol, a series of new peaks at 293.5 (CF_3), 291.2 (CF_2), 290.6 (CF_2 beside CH_2), and 284.9 eV (aliphatic carbon) were observed. This was confirmed by the presence of an intense peak at 688.5 eV in the F 1s spectrum of this sample (data not shown).

A summary of the normalized atomic elemental composition of each sample is shown in Table 1. The changes in the carbon signal after each step were analyzed in greater detail. In Figure 4, the ratio I_{C1s}/I_{Au4f} after each step are presented. As can be seen, this ratio strongly decreases after the UV illumination step. This may be linked to a minor degradation of the alkyl chains on the dodecanethiol during the process, which reduces the number of carbon atoms in the alkyl chains. A further decrease happens after rinsing with ethanol, meaning that some of the sulfonates species are removed, as described above in the discussion on the S 2p signals. After backfilling with 11-mercapto-1-undecanol or the perfluorinated thiol, the layer is restored and the ratio increases again. A smaller ratio is however observed when backfilling with the perfluorinated thiol. This lower carbon ratio can be partially explained by the smaller number of carbon atoms in the 1H,1H,2H,2H-perfluorodecanthiol than in 11-mercapto-1-undecanol.

Table 1. Elemental Composition Measured from the XPS Spectra of the SAM after Each Step of the Process[a]

	elemental composition (atom %)						
			O1s		S2p		
sample	Au 4f	C 1s	533.5 eV	531 eV	163 eV	168 eV	F 1s
1	44.2	52.7	0.0	0.0	3.1	0.0	0.0
2	52.4	35.2	3.2	6.8	0.3	2.0	0.0
3	76.9	20.1	0.1	2.1	0.6	0.2	0.0
4	45.4	45.9	5.7	0.2	2.8	0.0	0.0
5	29.7	24.0	0.0	0.0	1.5	0.0	44.8

[a] (1) Dodecanethiol SAM. (2) Following photocatalytic lithography. (3) Following photocatalytic lithography and ethanol rinsing. (4) Following photocatalytic lithography, ethanol rinsing, and backfilling in 11-mercapto-1-undecanol. (5) Following photocatalytic lithography, ethanol rinsing, and backfilling in 1H,H,2H,2H-perfluorodecanethiol.

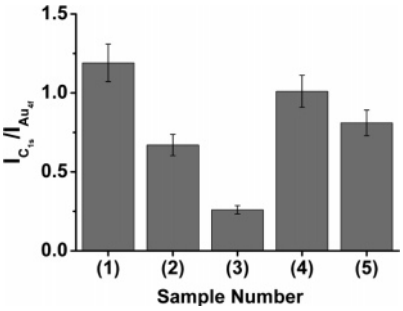

Figure 4. C 1s intensity divided by substrate intensity (Au 4f) measured after the five subsequent preparation steps. A clear reduction of the signal can be observed after (2) UV irradiation and (3) subsequent ethanol rinsing. The layers are restored by backfilling with (4) 11-mercaptoundecanol or (5) perfluorinated thiol, respectively. Error bars were estimated from the signal-to-noise ratios.

The results obtained from contact angle and XPS measurements suggest a potential degradation mechanism of the thiol monolayer. One clear aspect is the formation of sulfonate species due to the oxidation of thiols, which has been reported in many studies.[20,25,26] In parallel to thiol oxidation, some oxidation of the alkyl chains is happening. After the ethanol rinsing step, only the sulfonate species are removed from the SAM. This leads to an incomplete thiol SAM on the surface. During backfilling, the vacant sites exposed by the ethanol rinse are occupied by new thiol molecules, completing the SAM once more.

To fabricate a surface-chemical gradient, the TiO_2 layer was illuminated with a spatial gradient in UV intensity. Because the photocatalytic activity of TiO_2 depends on the intensity of UV light illumination,[16] the number of radicals created on the TiO_2 surface varied along the gradient. The SAM was therefore oxidized in a gradient. After the ethanol rinse step, the SAM was backfilled with the 11-mercapto-1-undecanol to obtain a more complete SAM exhibiting a composition gradient as illustrated in Figure 1. As shown in Figure 2, the gradients obtained were not linear, which may be undesirable for some practical applications. This issue is, however, readily addressed in our case by designing a nonlinear gray-tone gradient that would compensate for the nonlinearity of the process. The strength of this technique is

(21) Willey, T. M.; Vance, A. L.; van Buuren, T.; Bostedt, C.; Terminello, L. J.; Fadley, C. S. *Surf. Sci.* **2005**, *576*, 188−196.
(22) Harker, H.; Sherwood, P. M. *Philos. Mag.* **1973**, *27*, 1241−1244.
(23) Kubo, W.; Tatsuma, T. *J. Mater. Chem.* **2005**, *15*, 3104−3108.
(24) Zürcher, S.; et al. *J. Am. Chem. Soc.*, to be submitted for publication.
(25) Tarlov, M. J.; Burgess, D. R. F.; Gillen, G. *J. Am. Chem. Soc.* **1993**, *115*, 5305−5306.
(26) Dishner, M. H.; Feher, F. J.; Hemminger, J. C. *Chem. Commun.* **1996**, 1971−1972.

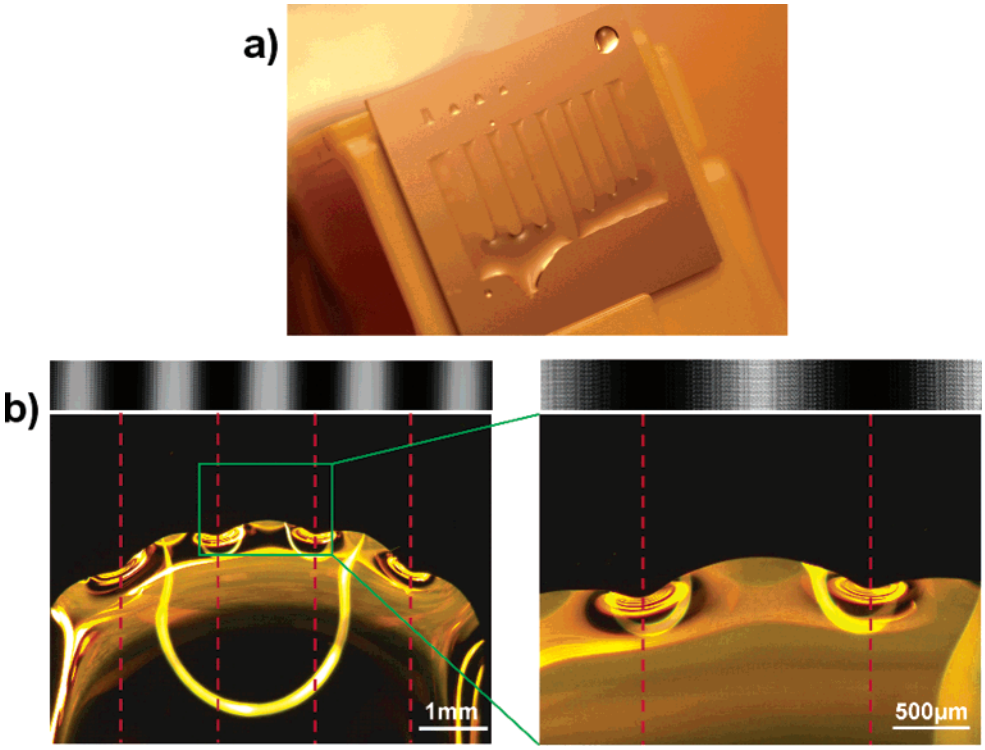

Figure 5. (a) Optical image of ethanol dewetting following photocatalytic lithography. (The sample was 1.5 cm wide.) (b) Dark-field images of a water droplet deposited on the surface bearing the repeating 720 μm gradients. The corresponding grayscale variations are shown above each image.

indeed its flexibility because the shapes, lengths, and slopes of the gradient may be adjusted at will by modifying the gray-tone gradients.

The final gradient of oxidized species will also depend on the photocatalysis parameters. Unfortunately, the underlying process of photocatalytic remote oxidation is not yet fully understood. The generation of radicals at the TiO_2 surface has been the subject of many studies.[27,28] It is well accepted that the main radicals created at the TiO_2 surface in the presence of oxygen are hydroxyl ($HO^{\bullet}$) and superoxide radicals ($O_2^{\bullet-}$ and $HO_2^{\bullet}$). The generation of such radicals depends on the physical and chemical characteristics of the TiO_2 nanoparticles. As already reported in literature,[29] the size of the nanoparticles is important: smaller nanoparticles lead to a larger surface area, which increases the number of surface-active sites and thus the number of radicals generated. However, a decrease in particle size also means a higher rate of electron−hole recombination,[30] which is detrimental to the photocatalytic process. It has been found that there is actually an optimal nanoparticle size, corresponding to 10 nm, at which the highest photocatalytic efficiency is achieved.[29] Another critical aspect is the nanoparticle surface chemistry. Several studies have reported that the density of hydroxyl groups on the TiO_2 surface plays an important role in the photocatalytic process.[29] To have reproducible surface chemistry, the TiO_2 surfaces used in this study were subjected to oxygen plasma cleaning followed by UV exposure. One last important parameter is the crystallinity of the nanoparticles. It is well known that the brookite and rutile TiO_2 phases have lower photocatalytic efficiency than does the anatase form.[23] In our case, we used nanoparticles of anatase TiO_2 that were 7 nm in diameter.

The last part of this work concerns the fabrication of submillimeter wettability gradients. The method described above was repeated using the 720 μm gray-tone gradient. However, characterization could not be performed by means of standard contact-angle measurements because of the small gradient size. Instead, the wetting properties of ethanol and water on the gradients were used to obtain a qualitative view of the gradient (Figure 5). Upon dipping the samples in ethanol after photocatalytic remote oxidation, ethanol dewetted from the hydrophobic areas of the sample but wetted the hydrophilic, oxidized regions. Because the gradient was periodic, this led to stripes of ethanol. As mentioned above, no significant effect on the water contact angle was observed immediately following photocatalytic remote oxidation. However, after rinsing with ethanol and backfilling with 11-mercapto-1-undecanol, the shape of a sessile water drop revealed the wettability changes along the gradient (Figure 5c). On the hydrophobic regions, the drop dewetted more than on the hydrophilic areas. Because the short wettability gradients repeated along the sample, this resulted in the formation of a wavelike triple line. The shape of the sessile drop demonstrates that this technique allows the wettability of the substrate to be modified on the submillimeter scale.

The limits of lateral resolution in this technique will determine the minimal gradient length achievable. The gradient in chemistry is here obtained from a gradient in UV-light intensity. The length of the gray-tone gradient used for that was 720 μm. The first limitation is linked to the fabrication of a gray-tone gradient on a smaller scale. We used standard photolithography processes that may not be suitable for the fabrication of gradients smaller than 10 μm. To overcome this problem, the photomask could be fabricated, for instance, using an e-beam pattern generator and high-energy-beam-sensitive glass (HEBS).[31] The problems of resolution in photocatalytic lithography have already been

(27) Lee, N. C.; Choi, W. Y. *J. Phys. Chem. B* **2002**, *106*, 11818−11822.
(28) Ishibashi, K.; Nosaka, Y.; Hashimoto, K.; Fujishima, A. *J. Phys. Chem. B* **1998**, *102*, 2117−2120.
(29) Carp, O.; Huisman, C. L.; Reller, A. *Prog. Solid State Chem.* **2004**, *32*, 33−177.
(30) Zhang, Z.; Wang, C. C.; Zakaria, R.; Ying, J. Y. *J. Phys. Chem. B* **1998**, *102*, 10871−10878.

addressed by Kubo et al.[15] These authors used photocatalytic lithography to make surface patterning and reported resolutions of 10 μm. The fabrication of shorter gradients than described here can thus be envisaged. A final limitation arises from the lateral diffusion of the radicals through the 60 μm air gap. The resolution could readily be improved by decreasing the air gap between the TiO_2 layer and the substrate. Reducing the gap significantly below that used in the current work would, however, necessitate using clean-room conditions because of the possibility of dust lodging in the air gap and giving a nonreproducible and nonuniform gap.

Conclusions and Outlook

Both centimeter- and submillimeter-long surface-chemical gradients have been obtained using a simple technique that combines photocatalytic and grayscale lithography. The creation of surface-chemical gradients was demonstrated by gradually degrading alkanethiol SAMs and backfilling to produce wettability gradients. The technique may be applied to other combinations of thiol end-groups or, indeed, to other surface chemistry entirely. To date, the modification of surface wettability by photocatalytic lithography has also been shown for systems such as silane SAMs and some polymer surfaces,[23] correspondingly increasing the possible range of applications.

The shape and length of the gradients are controlled via the design of the grayscale gradient on the photomask. This approach may easily be extended to other gradient shapes (for instance, radial gradients) and other gradient slopes simply by using a different photomask. One interesting point is the size of the shortest gradient that can be obtained: previous studies using photocatalytic lithography to pattern surfaces reported resolutions of 10 μm[15], which suggests that gradients approaching such scales may be feasible.

The chemistry of the lithographic process has not yet been fully elucidated. However, several parameters are expected to influence the final gradients, such as the precise structure and chemistry of the TiO_2 layer, the humidity of the ambient air,[27,32] and the size of the air gap between the substrate and the photocatalytic layer.[33] Optimization of these parameters should allow better control of the final chemical gradient shape, slope, and resolution.

Acknowledgment. We thank Dr. Emmanuel Scolan and Dr. Rolf Steiger for useful scientific discussions. We also acknowledge Arrayon Biotechnology, Dr. Harry Heinzelmann, and Dr. Raphaël Pugin for their support of this work.

LA063186+

(31) Däschner, W.; Long, P.; Stein, R.; Wu, C.; Lee, S. H. *Appl. Opt. IP* **1997**, *36*, 4675−4680.

(32) Kozlov, D. V.; Panchenko, A. A.; Bavykin, D. V.; Savinov, E. N.; Smirniotis, P. G. *Russ. Chem. Bull.* **2003**, *52*, 1100−1105.

(33) Tatsuma, T.; Tachibana, S.; Miwa, T.; Tryk, D. A.; Fujishima, A. *J. Phys. Chem. B* **1999**, *103*, 8033−8035.